Journal of Materials Processing Technology 155–156 (2004) 1881–1888

Journal of Materials Processing Technology

www.elsevier.com/locate/jmatprotec

The cooling process in gas quenching

N. Lior[a,b,*]

[a] *Department of Mechanical Engineering and Applied Mechanics, University of Pennsylvania, 297 Towne Building, 220 South 33rd Street, Philadelphia, PA 19104-6315, USA*

[b] *Faxénlaboratoriet, Kungl. Tekniska Högskolan, Stockholm, Sweden*

Abstract

Gas quenching is a relatively new process with several important advantages, such as minimal environmental impact, clean products, and ability to control the cooling locally and temporally for best product properties. To meet the high cooling rates required for quenching, the cooling gas must flow at very high velocities, and such flows are highly turbulent and separated. Consequently, there is a need for good understanding of these flows and their consequences for the process. To that end, we researched the state of the art, and have conducted numerous numerical and experimental studies and developed CFD models on this subject, and show the results for flows inside quench chambers and their components, and for external flows, including multi-jet impingement, on cylindrical and prismatic single and multiple bodies (the quench charge). Velocity distributions and uniformity, pressure drop, and flow effects on heat transfer coefficients and product uniformity, as well as recommendation for improved processes, are shown.

Keywords: Gas quenching; Heat treatment; Flow modelling; Solid phase transformations

1. Introduction

The use of gas instead of liquid as quenchant has environmental, product quality, process control, safety and economic advantages (cf. [1]) and its improvement is under intensive study at the Faxén Laboratory of the Royal Institute of Technology, Sweden (cf. [2–15]) and elsewhere (cf. [16]). The primary effort is focused on finding ways to generate sufficiently high heat transfer coefficients, and to produce cooling which results in minimal distortions and most uniform mechanical properties of the quenched parts. A review of the cooling process in gas quenching, including flow in quench chambers, furnaces, and their components, and cooling of single and multi-body quench charges is presented, with emphasis on the fluid mechanics and heat transfer aspects. The state of the art can also be found in the citations contained in the quoted references.

2. Flow inside quench chamber and their components

2.1. Quench chambers and furnaces

The high gas velocities and pressures required for gas-cooled quenching dictate careful design of the flow passages to assure good flow distribution across the charge, and to minimise the flow pressure drop. We have conducted studies ([2,3]) with the objectives to (1) investigate the reasons for flow nonuniformity in gas quenching chambers and develop ways for their alleviation, and (2) develop computational fluid mechanics tools for simulating the flow in such chambers. A scale model of such a chamber was constructed, and detailed experimental studies of the flow in it were conducted. A numerical program, adapting commercially available software, was developed to simulate the flow in cold gas quenching chambers of complex configuration. The model was successfully validated by comparison with the experimental data we have obtained from the scale model. The geometry of such a chamber is shown in Fig. 1, where (1) is the gas inflow from blower; (2) upflow, split into two streams; (3) flow direction reversal and merger; (3–4) the quench charge zone; (4) gas exhaust, split. The velocity distribution is shown in Fig. 2, where there is also a comparison of the results for the gas assumed as compressible to those where it is assumed incompressible. Only one half of the quench chamber is shown due to symmetry. The fastest downflow in the central duct is at the centerline; note recirculation eddies next to the charge zone wall.

The flow distribution for nitrogen at the extreme conditions considered in this analysis, 50 bar, with an average velocity of 30 m/s in the charge zone, is shown in Fig. 2. The flow is seen to converge towards the centre as it reverses

* Tel.: +1-215-898-4803; fax: +1-215-573-6334.
E-mail address: lior@seas.upenn.edu (N. Lior).

0924-0136/$ – see front matter © 2004 Elsevier B.V. All rights reserved.
doi:10.1016/j.jmatprotec.2004.04.279

Nomenclature

AL	duct length ratio, L/D, dimensionless
AR	duct flow cross-section aspect ratio, a/b, dimensionless
A_s	Surface area of a quenched body, m^2
Bi	Biot number, hL_c/k_s, dimensionless
d	jet nozzle diameter
D	Characteristic dimension of a duct, such as diameter, m
Fo	Fourier number, $\alpha\tau/L_c^2$, dimensionless
h	convective heat transfer coefficient, $Wm^{-2}\,K^{-1}$
H	gap between jet nozzle outlet and cooled body surface, m
k	thermal conductivity, $Wm^{-1}\,K^{-1}$
L	duct length, m
L_c	characteristic dimension of a quenched body
N	velocity nonuniformity criterion, $N = (1/u_{av})\iint_s (1/S)(u-u_{av})^2\,dS$, dimensionless
Nu	Nusselt number, hL_ck^{-1}, dimensionless
P	pressure, Pa or bar
Pr	Prandtl number, ν/α, dimensionless
q_c	overall convective heat loss rate from the surface of a quenched body, W
Re_D	Reynolds number based on characteristic dimension D ($uD\nu^{-1}$)
S	cross-sectional duct flow area, m^2
t	pitch between jet nozzles, m
T	temperature, K
Tu	free stream turbulence intensity, %
u	velocity, ms^{-1}
V	volume of quenched body, m^3

Greek symbol

α	thermal diffusivity, $m^2\,s^{-1}$
Γ	a quenching uniformity figure of merit, $\Gamma \equiv \dot{q}_c(A_s/V)^2/(k_s\lvert\overline{\nabla T}\rvert)$
ν	kinematic viscosity, $m^2\,s^{-1}$
τ	time, s
$\lvert\overline{\nabla T}\rvert$	the volumetric average of the absolute temperature gradients in the quenched body

Subscripts

av	average
s	solid, or surface

direction after hitting the lid at the top. It forms a high speed core downflow, reaching at the duct centre a velocity up to about four times the average, as well as a large accompanying recirculation eddy which has a downward flow direction near the downflow core and an upward flow direction near the wall.

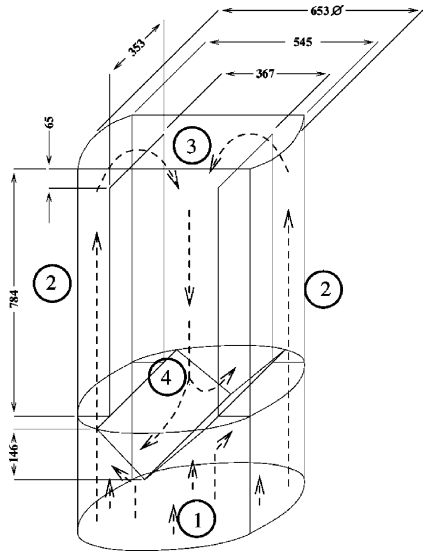

Fig. 1. The configuration and main dimensions (in mm) of the experimental chamber, and the air flow directions in it [2].

For all gases at all the pressures the downflow width (between the side-walls) was about 61–62% of the total flow width, increasing within this range with the flow Reynolds number, as shown in Fig. 3. Noting from Fig. 3 that even this downflow has a severe flow variation in the horizontal direction, this clearly indicates that the chamber design is poorly suitable for heat treatment.

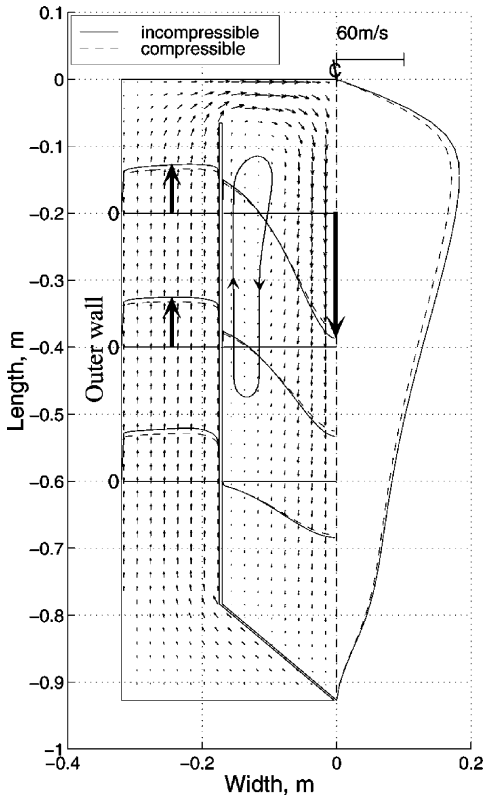

Fig. 2. The computed flow distribution in the chamber, for flow of nitrogen at 50 bar, 20 °C, and average velocity of 30 m/s in the charge zone [2,3].

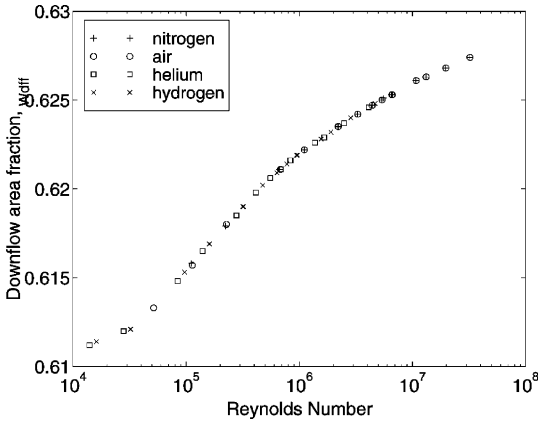

Fig. 3. The fraction of the charge zone width in which there is downflow (computed at 0.227 m under the lid), as a function of the Reynolds number, for all the gases [3].

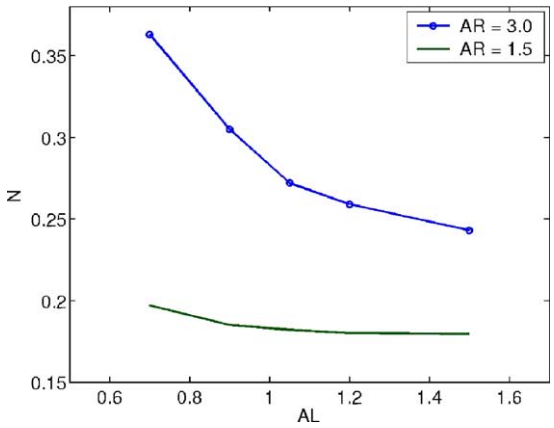

Fig. 4. Effect of circular-to-rectangular cross-section transition length on velocity nonuniformity, $P = 1$ bar, $T = 298.3$ K, $Re_D = 5.9 \times 10^5$, [4].

Some of the main conclusions about flow in quench chambers are:

- The velocity nonuniformity is nearly independent of the type of gas.
- The flow characteristics and overall pressure drop are nearly independent of the gas temperature in the temperature range considered.
- The flow nonuniformity is caused primarily by the flow pattern dictated by the chamber design, where upflow gas streams are reversed in direction and merged before their entrance to the charge zone.
- The employment of a perforated plate at the entrance to the charge zone, as used in one commercial design, does eliminate the recirculation eddies but still leaves a highly nonuniform downflow and increases the overall pressure drop by more than 45%. With the same inlet pressure, the latter effect causes, however, the velocity to decrease to half of its value when this plate was not employed.

2.2. Quench chamber and furnace components

The flow ducting geometry in quench chambers is often rather complex (cf. Fig. 4), with flow splitting, 90–180° bends, and circular-to-rectangular cross-section (or other shapes) transition ducts (the latter are used, for example, between the circular blower duct and the rectangular quenching baskets). Similar situations exist in forced convection furnaces. To provide design guidance in the choice of such ducts, and focusing primarily on circular-to-rectangular transition ducts, the flow was modelled and computed. Sensitivity of the velocity uniformity and pressure drop to the primary geometric parameters, pressure, and Reynolds numbers was examined, with an ultimate objective to produce optimal designs. Low length-to-(inlet diameter) ratios (cf. Fig. 4) and high exit cross-section aspect ratios were shown to increase both distortion of the exit velocity field and the overall pressure drop. Expanding–contracting transition ducts were seen to improve flow uniformity. Further details are available in [4] in this issue.

3. The relationship between the cooling flow field and the temperature distribution inside quenched bodies

The temperature distribution uniformity and the magnitude of the temperature gradients in the quenched solid have a primary effect on distortions and residual stresses. On the path to determine the effect of the cooling gas flow on these undesirable phenomena, it is thus easier and rather useful to first find the sensitivity of these temperature distributions and gradients to the surface heat transfer coefficient distribution. The temperature distributions in two practical body shapes, a long cylinder and a long rod with a square cross-section, subjected to several convective heat transfer coefficient distributions have thus been computed [5]. Large temperature gradients were found, especially, as expected, near the body surfaces and corners. In addition, the volume-average of the absolute values of the temperature gradients, and a heat treatment figure of merit, $\Gamma \equiv \dot{q}_c \, (A_s/V)^2 \, / (k_s |\overline{\nabla T}|)$, that we have defined, have been calculated. In heat treatment it is typically desirable to have high overall cooling rates yet low temperature gradients, thus higher values of Γ imply a better heat treatment process. Similarly, a higher surface-to-volume ratio is more desirable in quenching, and it was raised in this definition to the second power so that Γ would become dimensionless.

We note that while temperature gradients have a primary role in generating distortions, residual stresses and problems with the final mechanical properties of the quenched object, due to thermal stresses and peculiarities in the crystalline phase transformations, these undesirable effects are affected by other parameters too (cf. [6–8]).

Γ was found to increase with increased uniformity of h, and to decrease with time during the cooling period.

More about the relationship between the cooling flow field and the steel property consequences is presented in Section 4.1 below.

4. Convective cooling of bodies

4.1. Single bodies, unidirectional flow

4.1.1. Single round cylinders in cross flow

A k-ε turbulent flow and heat transfer model was adopted ([5–8]) to predict the h distribution over cylinders. In comparison with available experimental data, it was found to be much better than two of the most popular ones in use, but still may have local errors of up to about 40%. To illustrate the cooling nonuniformity problem, Fig. 5 shows the flow, heat transfer and nonuniformities as computed by this model for cross-flow quenching of a steel cylinder. The boundary layer thickens from the stagnation point downstream, until separation is seen to occur at about the azimuthal angle of 100°, followed by a recirculation zone and wake. As expected, h is seen to be high in the stagnation region, gradually decreasing downstream as the boundary layer thickens, rising to a maximum in the flow separation region, then decreasing, and slightly increasing in the wake region further downstream.

This model, as well as available experimental and representative data (cf. [9,10]), were used to define the distribution of the convective heat transfer coefficient around the body surface as the boundary condition of a heat treatment simulation code developed at the Swedish Institute for Metals Research [6–8]. It can be used for prediction of temperature, microstructure, stresses and distortion of quenched steel bodies. A direct dependence of the distortion on the extent of convective heat transfer nonuniformity was established for bearing steel tubes and solid cylinders, and an example of the results is shown in Fig. 6. As seen and expected, surface zones at which h is higher are where the body contracts as a consequence of quenching, and v.v.

Some of the other conclusion are that (1) the magnitude of the maximal temperature gradient in the quenched body is highly sensitive to the local magnitude of h, hence affecting mechanical properties, (2) if the hardenability is not large enough to produce a fully martensitic microstructure, the nonuniform heat transfer will also result in nonuniform microstructure and other nonuniform properties such as hardness, as well as lead to additional distortion from mixtures/distributions of constituents with different specific volumes, and (3) the magnitude and distribution of the convective heat transfer coefficients at the surface of the quenched piece have a significant effect on its distortion and mechanical properties.

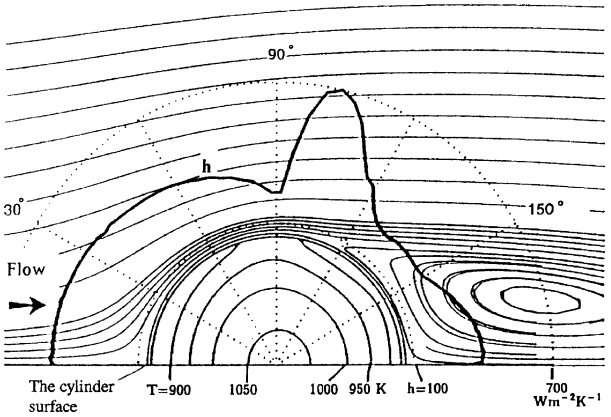

Fig. 5. Typical streamlines, surface heat transfer coefficient (h) and internal temperature (T) distribution as computed for the crossflow quenching of a stainless steel cylinder. Initial cylinder temperature = 1200 K, quenching gas (nitrogen) temperature = 300 K, P = 10 bar, k_s = 20 $Wm^{-1}K^{-1}$, $Re = 0.316 \times 10^6$, $Pr = 0.7$, $Bi = 0.66$, $Fo = 0.27$ [8].

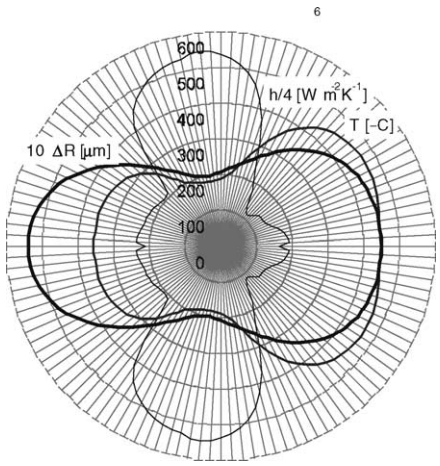

Fig. 6. Polar diagrams of heat transfer coefficients h, surface temperature T and outer radius change ΔR. The temperature is given after 7 s for $Re = 1.0 \times 10^6$ [8].

4.1.2. Single square cylinders in cross flow

Local Nusselt numbers on the surfaces were evaluated from the measured surface temperatures using a thermochromic liquid crystal (TLC) technique [9–12], and the velocity distributions around the test bodies were measured using particle image velocimetry (PIV), on single quadratic cylinders, for attack angles of $\alpha = 0°$ and 45° with respect to the upstream flow. Re was varied from 39,000 to 116,000, and the upstream free stream turbulence was <0.04%.

Fig. 7 shows a velocity distribution around a cylinder. Typical is the fairly attached flow at the front surface,

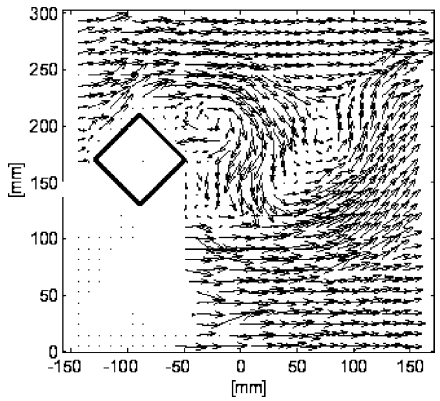

Fig. 7. Instantaneous velocity field, single cylinder, flow angle of attack = 45°, cross flow (from left) Re_D = 78,000 [11].

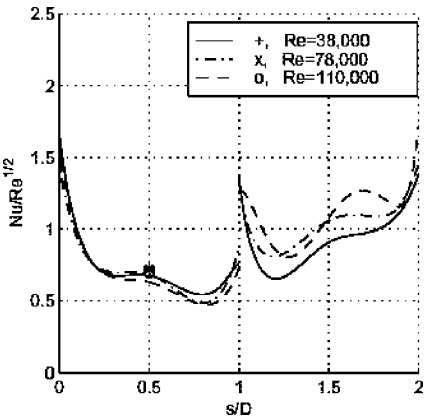

Fig. 8. Scaled *Nu* distributions for a single cylinder of side *D*, at different *Re*, flow angle of attack = 45° [11]. The abscissa *s*/*D* indicates locations along the surface = 0 at left-most corner = 1 at top corner = 2 at rear corner. Symbols: independent measurements using thermocouples.

separation at the upper corner, and highly complex wake flow. Following that flow pattern, *Nu* is seen in Fig. 8 to decay downstream from a maximum at the front corner, and closer to the middle corner it starts to increase again (note: the trends and values shown in this figure and Fig. 11 are at least approximately correct, but are still being validated). *Nu* for the rear surfaces were in average 1.26–1.62 times higher than for the front surfaces in this range of *Re*. The local *Nu* was in general increasing from the middle corner towards the rear corner. It is obvious from the results that *Nu* varies by about three-fold along the cylinder surface, typically peaking at the front attachment point and at the corners.

4.1.3. Single round cylinders in axial flow

Convective heat transfer coefficient information for high *Re* in such flow configurations is nearly unavailable, so the local heat transfer coefficient distributions on a two-diameter long cylinder (150 mm in diameter) was measured in axial flows of air, at Reynolds numbers (*Re*) of 8.9×10^4 to 6.17×10^5 (9–63 m/s) [12]. The measurements were performed at different upstream flow turbulence level (*Tu*) using a turbulence-generating grid, and by using flow modification inserts in front of the cylinder. The heat transfer coefficients were evaluated from the measured surface temperatures on the cylinder round envelope, and the flat ends, using a thermochromic liquid crystal (TLC) technique.

The results are shown in Fig. 9. On the front (upstream) surface of the cylinder, a–b, the heat transfer profiles are almost flat. The average of *Nu* is significantly higher along the surface b–c, on which a maximum of roughly double the value at surface a–b, was found at 0.9*D* from the front edge. On the rear surface c–d, *Nu* drops to a value 30–50% lower than that at a–b, increasing from the edge. The averages along the whole surface a–d, were for these three Reynolds numbers found to be $Nu_{a–d} = 803$, 535, and 337, respectively. Similar to the result for cylinders in cross flow, *Nu* varies by about three-fold along the cylinder surface, but here peaking along the round surface (b–c).

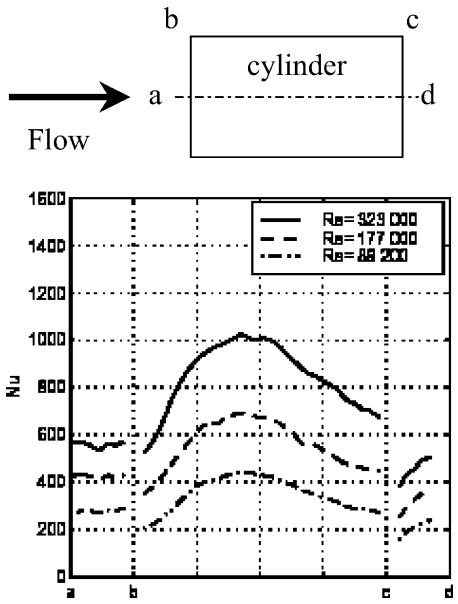

Fig. 9. *Nu* distribution along the cylinder surface in axial flow for three *Re*; *Tu* = 6.7% [12].

Relative to the flow with very low free stream turbulence (*Tu* = 0.3%), increasing *Tu* to 6.7% caused an increase in the heat transfer coefficient up to 22% and when a flow modification insert was used the nonuniformity was reduced up to 35%. Correlations between *Nu* and *Re*, in the form $Nu = CRe^e$ were developed for all of the cylinder surface, where *c* and *e* are empirically fitted coefficients.

4.2. Multiple bodies, unidirectional flow

More often than not, quench charges are composed of groups of parts, loaded as such into a quench chamber. Obviously, the flow at any one of these parts is affected strongly by the presence of other parts in that charge, and it is important to understand that interaction and its effect on local and overall cooling rates. Some of our experimental results are shown and discussed here.

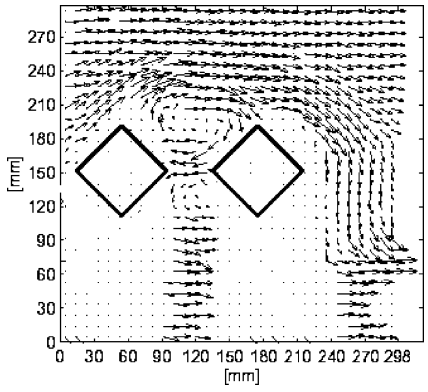

Fig. 10. Instantaneous (instant when the flow is bypassing the cylinders) velocity field around two cylinders in a row, at distance $p = 2D$, flow angle of attack = 45°, *Re* = 78,000 [11].

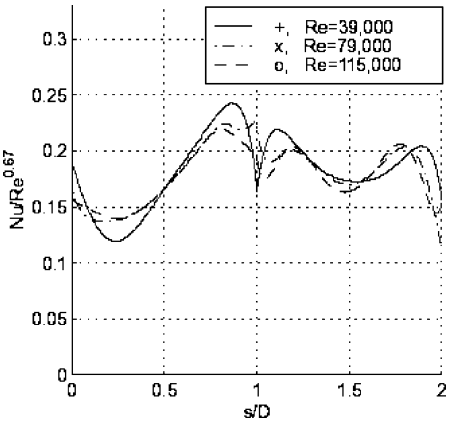

Fig. 11. Scaled Nu_{av} for the second of two cylinders in a row at different *Re*, distance $p = 2D$, flow angle of attack = 45° [11].

The local Nusselt numbers on the surfaces together with the velocity distributions around the test bodies, were evaluated from TLC measurements performed on quadratic cylinders, in different configurations, for attack angles of 0° and 45° with respect to the upstream flow direction [11]. *Re* was varied from 39,000 to 116,000, while the upstream free stream turbulence (*Tu*) was <0.04%. The configurations included two, three, four, and five cylinders, as partially shown below, with different pitches. It is obvious from the results that *Nu* varies by about three-fold along the cylinder surface, similar to the ratio with single cylinders, typically peaking at the front attachment point and at the corners.

For two cylinders in a row, flow angle of attack = 45°. Fig. 10 shows that the second cylinder is subject to wake flows from the first cylinder, which are found to be periodic (about 50 Hz), with the flow going for some instance up, another instance down, and yet for another almost bypassing the inter-cylinder gap. The nature of this oscillating and vigorous flow generates higher average *Nu* for the downstream cylinder than was found for a single cylinder. As seen in Fig. 11, the *Nu* varies along the surface by about two-fold. Increasing the inter-cylinder pitch from 2*D* to 4*D* decreased the average *Nu* on the downstream cylinder, but only slightly.

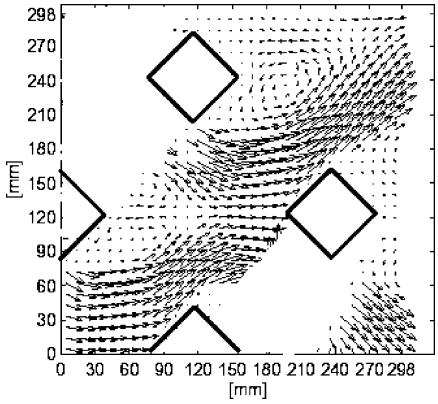

Fig. 12. Average velocity data around four cylinders, pitch = 2*D*, flow angle of attack = 45°, *Re* = 78,000 [11].

The flow between and around a bank of four cylinders in a square arrangement and flow angle of attack = 45° is shown in Fig. 12. Nu_{av} on the rear surface of the downstream cylinder was 0.67 of the value on the front surface.

It is noteworthy that Nu_{av} is highest for the downstream cylinder in a two-cylinder bank, becomes lower for the downstream cylinder in a four-cylinder bank, and is lowest for the central cylinder in the five-cylinder bank. Another important conclusion is that the upstream cylinder cooling differs significantly from that of those downstream, which experience, on the average, much closer cooling rates.

5. Multi-jet impingement quenching

Due to the high heat transfer coefficients it produces, jet impingement, which is increasingly used in industry to cool, heat or dry a surface in applications such as cooling of gas turbine components, drying of textile, film and paper, and annealing of metal and plastic sheets, is of interest here. It has been the topic of many papers and several reviews; the most relevant ones to this study being those by Martin [17] and Viskanta [18]. The study of such cooling remains intensive.

A commercial nozzle-field gas quenching system is presented in Fig. 13 [13,14]. After austenitization, the rings are placed one at a time in the device for quenching. The air (or nitrogen) at approximately atmospheric pressure is blown into the device. The air passes at high speed through the inner and the outer nozzle fields and impinges on the inner and outer faces of the rings. It then exits the device in the upward and downward directions. The ring lies on a rotating base, which makes it spin, improving the uniformity of the cooling.

A number of empirical formulas available for computing multi-jet impingement cooling heat transfer coefficients were evaluated, and Martin's formula [17] was found to be most suitable.

To estimate whether the convective heat transfer coefficients predicted by this formula are sufficiently high to produce a fully martensitic transformation during quenching,

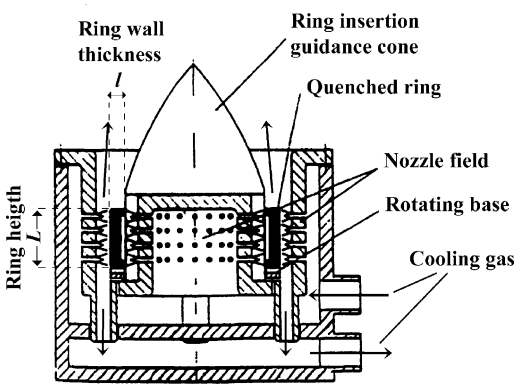

Fig. 13. A nozzle-field gas quenching device for rings [14].

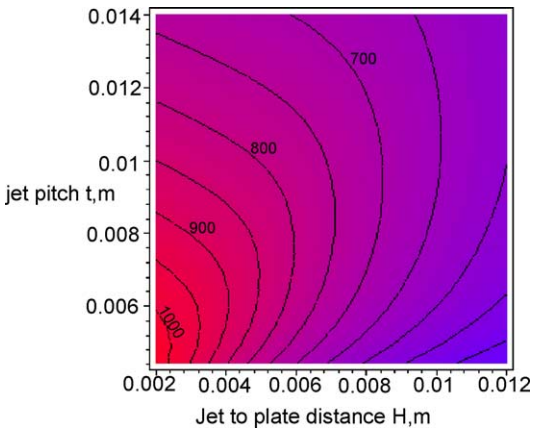

Fig. 14. Constant heat transfer coefficient, h, contours in $\mathrm{Wm^{-2}\,K^{-1}}$, as a function of H and t for $d = 0.001$ m, inline jet arrangement and constant blower power [14].

two numerical models have been developed: (1) a transient heat conduction model to compute the temperature field history in an austenitic body during quenching, and (2) a phase transformation model to estimate the transformation of austenite to pearlite and bainite occurring during quenching as a function of temperature. Combining these models, computations were made for various steel ring sizes to determine the h needed to quench a ring for a certain transformation fraction [13,14]. This is another example of how one can estimate the convective heat transfer information for attaining a desired level of phase transformation in quenching.

There are many multi-jet impingement cooling parameters that can be changed to improve the heat transfer rates. Addressing the spatial arrangement of the nozzles and their distance to the ring, optimisation was conducted to maximise the convective heat transfer coefficient, which was obtained for $d = 0.184H$, $t = 1.423H$ for staggered arrays of nozzles, or $t = 1.324H$ for an inline arrays of nozzles. Assuming maintenance of constant blower power, a sensible engineering assumption. Fig. 14, for example, shows that the highest h is obtained for the smallest values of H and t for these conditions.

Other optimisation results and a number of recommendations were proposed in [14] for improvements of multi-jet quenching devices.

6. Summary and conclusions

A review of gas quenching flow and heat transfer, inside quench chambers and their components, and for external cooling flows, including multi-jet impingement, on cylindrical and prismatic single and multiple bodies (the quench charge) was presented.

The flow nonuniformity in quench chambers is caused primarily by the chamber design. Hence, uniformity, as well as pressure drop can be controlled by proper design of the flow passages. This can be most effectively done by preliminary CFD modelling and simulation. When designing ducts with flow area changes, low length-to-(inlet diameter) ratios and high exit cross-section aspect ratios increase both distortion of the exit velocity field and the overall pressure drop.

In unidirectional cross- or axial-flow cooling of round or square cross-section cylinders, variations in the heat transfer coefficient of up to about three-fold occur along the cylinder surface. These nonuniformities are somewhat diminished by increasing the upstream free stream turbulence intensity.

Obviously, knowledge of the heat transfer coefficient distribution along the quenched part surface allows, in conjunction with solid mechanics and phase transition modelling of the quenched part, the prediction of extent of phase transformation, mechanical properties, and distortion of the part. This was indeed done, indicating that distortion and property-nonuniformity are somehow proportional to the nonuniformity in the surface heat transfer coefficient.

In a charge composed of a number of cylinders, the upstream cylinder cooling differs significantly from that of those downstream, which experience, on the average, much closer cooling rates. The cooling depends in general on the specific location of the part.

High and uniform heat transfer coefficients can be obtained in multi-jet impingement cooling, and this process can be optimised by the design of the impingement system and its adaption to the specific parts that are being quenched.

Acknowledgements

This work was performed by the Faxénlaboratoriet of the Kungl. Tekniska Högskolan (KTH), Stockholm, and partially sponsored by LindeGas GmbH (formerly AGA AB), Ipsen International GmbH, SKF Engineering and Research Center, B.V., and Volvo Personvagnar Komponenter AB.

The results are based on work by the past and current students Jerome Ferrari, Nulifer Ipek, Mats Lind, Olivier Macchion, Alberto Stroppiana, and Roland Wiberg. The author is grateful for their important contributions and for the participation and encouragement of the Faxénlaboratoriet Director, Professor Fritz Bark, and Scientific Coordinator Dr. Michael Vynnycky.

References

[1] S.J. Midea, T. Holm, S. Segerberg, J. Bodin, T. Thors, K. Swartström, High pressure gas quenching—technical and economic considerations, in: Proceedings of the Second International Conference on Quenching and the Control of Distortion, ASM International, 1996, p. 157.

[2] J. Ferrari, N. Ipek, N. Lior, T. Holm, Gas quench vessel efficiency: experimental and computational analysis, in: Proceedings of the 18th ASM International Heat Treating Society Conference, Rosemont, IL, 1998, pp. 500–505.

[3] J. Ferrari, N. Ipek, N. Lior, T. Holm, Flow considerations in quenching vessels, in: Proceedings of the Third ASM International Confer-

ence on Quenching and Control of Distortion, Prague, Czech Republic, 1999, pp. 93–101.
[4] O. Macchion, N. Lior, A. Rizzi, Computational study of velocity distribution and pressure drop for designing gas quench chamber and furnace ducts, in: S. Hashmi (Ed.) AMPT 2003, J. Mater. Process. Technol. 155–156 (2004) 1727–1733.
[5] M. Lind, N. Lior, F. Alavyoon, F. Bark, Flows effects and modeling in gas-cooled quenching, in: Proceedings of the 11th International Heat Transfer Conference on Heat Transfer, Korea, vol. 3, 1998, pp. 171–176.
[6] A. Thuvander, A. Melander, M. Lind, N. Lior, F. Bark, Prediction of convective heat transfer coefficients and examination of their effects on distortion of tubes quenched by gas cooling, in: Proceedings of the 11th Congress of the International Federation for Heat Treatment and Surface Engineering, 4th ASM Heat Treatment and Surface Engineering Conference in Europe, Florence, Italy, 19–21 October 1998.
[7] A. Thuvander, A. Melander, M. Lind, N. Lior, F. Bark, Prediction of convective heat transfer coefficients and their effects on distortion and mechanical properties of cylindrical steel bodies quenched by gas cooling, in: Proceedings of the Fifth ASME/JSME Joint Thermal Engineering Conference, San Diego, Paper AJTE99-6289, 15–19 March 1999.
[8] A. Thuvander, A. Melander, M. Lind, N. Lior, F. Bark, Prediction of convective heat transfer coefficients and their effects on distortion and mechanical properties of cylindrical tubes quenched by gas cooling, La Metallurgia Italiana XCI (4) (1999) 25–32.
[9] R. Wiberg, B. Muhammad-Klingmann, J. Ferrari, N. Lior, in: E.J. Mittemeijer, J. Grosch (Eds.), Use of Thermochromic Coatings for the Experimental Determination of the Distribution of Heat Transfer Coefficients in Gas-cooled Quenching, in: Proceedings of the Fifth ASM Heat Transfer and Surface Engineering Conference in Europe, ASM International, Gothenburg, Sweden, 7–9 June 2000, pp. 275–286.
[10] R. Wiberg, B. Muhammad-Klingmann, J. Ferrari, N. Lior, Thermochromic coatings help characterize gas quenching, ASM Int. Heat Treat. Prog. 158 (4) (2000) 37–40.
[11] R. Wiberg, Heat flux and velocity measurements on and around a single quadratic cylinder, and using groups of quadratic cylinders in the cross flow of air, Internal Report, Faxénlaboratoriet, Kungl. Tekniska Högskolan, Stockholm, Sweden, 2001.
[12] R. Wiberg, N. Lior, Convection heat transfer coefficients for axial flow gas quenching of a cylinder, in: Proceedings of the Fourth International Conference on Quenching and the Control of Distortion, Chinese Heat Treatment Society and ASM International, Beijing, 23–25 November 2003.
[13] J. Ferrari, N. Lior, J. Slycke, Gas quenching of steel rings by jet impingement, in: Proceedings of the ASM International and 13th International Federation for Heat Treatment and Surface Engineering Congress (IFHTSE/ISEC) 2002, Columbus, Ohio, 2002.
[14] J. Ferrari, N. Lior, J. Slycke, An evaluation of gas quenching of steel rings by multiple-jet impingement, J. Mater. Process. Technol. 136 (2003) 190–201.
[15] M. Vynnycky, J. Ferrari, N. Lior, Some analytical and numerical solutions to inverse problems applied to phase-transformation tracking gas quenching, ASME J. Heat Transfer 125 (1) (2003) 1–10.
[16] H.M. Tensi, A. Stich, G.E. Totten, Quenching and quenching technology, in: Steel Heat Treatment Handbook, Marcel Dekker, New York, 1997, Chapter 4, p. 157.
[17] H. Martin, Heat, mass transfer between impinging gas jets and solid surfaces, Adv. Heat Transfer 13 (1977) 1–60.
[18] R. Viskanta, Heat transfer to impinging isothermal gas and flame jets, Exp. Thermal Fluid Sci. 6 (1993) 111–114.